

*Scientific Note*

## **Application of He-microwave induced plasma atomic emission spectroscopy to an analysis of individual particulate matter**

Sanae Tamura<sup>1</sup>, Tadashi Kikuchi<sup>1</sup>, Hisao Takahara<sup>2</sup>,  
Minako Mishima<sup>2</sup> and Yoshiyuki Fujii<sup>3</sup>

<sup>1</sup>*Faculty of Science and Engineering, Science University of Tokyo in Yamaguchi,  
1-1-1 Daigaku-Dori, Onoda, Yamaguchi 756-0884*

<sup>2</sup>*Yokogawa Electric Corporation, 2-9-32 Nakacho, Musashino-shi, Tokyo 180-8750*

<sup>3</sup>*National Institute of Polar Research, Kaga 1-chome, Itabashi-ku, Tokyo 173-8515*

**Abstract:** He-microwave induced plasma atomic emission spectroscopy (He-MIP-AES) (H. Takahara, *Ultra Clean Technol.*, **5**, 310, 1993) has been used for the characterization of individual micro-particles. The GSJ (Geological Survey of Japan) geochemical reference samples, JB-1a (basalt, Sasebo, Nagasaki Prefecture), JB-3 (basalt, Mt. Fuji, Yamanashi Prefecture), and JR-1 (rhyolite, Wada Pass, Nagano Prefecture) were analyzed by He-MIP-AES. The major elements, Si, Fe, Ca, and Mg, and the minor elements, Cr and Ni, in these rock reference samples were chosen for analysis. We have directed our attention to the elemental compositions found from the correlation of simultaneous emissions especially. The JB-1a and JB-3 showed different characteristic correlation of simultaneous emissions between Fe and Mg, even though both of them are classified as basalt. This suggests that we can characterize micro-particles by measuring the correlation of simultaneous emissions for individual particles and analyzing the distinctive features of their correlation for all particles. Namely, the He-MIP-AES technique should be applicable for the identification of individual particulate matter, such as tephra particles.

### **1. Introduction**

An optical particle counter can provide the number of particles and the size distribution, but it does not indicate any information about chemical composition for identifying the origin. If we can obtain compositional data on each particle together with the size and number, we can identify the origin more accurately.

Bulk analysis of aerosol and tephra particles, such as atomic absorption spectrometry (AAS) and ion chromatography (IC) gives the average composition of all particles, but it does not provide any information on individual particles. On the other hand, microprobe analysis, such as scanning electron microscopy-energy dispersive X-ray analysis (SEM-EDX) shows the composition of individual particles. Kudo *et al.* (2000) attempted to use SEM-EDX for analyzing ice core particle samples taken from 384 m depth at Mizuho Station. However, SEM-EDX is not suitable for the analysis of light elements, even though the aerosol and tephra particles mainly consist of light elements. Meanwhile, laser microprobe mass spectrometry (LAMMS) indicates the

elemental and compositional information including light elements. Wouters *et al.* (1990) and Hara *et al.* (1996) applied LAMMS to analysis of Antarctic aerosol particles. However, these measurements have disadvantages such as inconvenient preparation, long analysis time, and the need for specialists to operate them.

In this study, He-microwave induced plasma atomic emission spectroscopy (He-MIP-AES) (Takahara, 1993) has been used to characterize individual particles. The He-MIP-AES provides all of the information, such as the particle number, the size ( "equivalent" particle diameter), and the elemental composition at the same time. In addition, the sample filter can be set in the instrument without any pretreatment and the sample micro-particles are delivered to the plasma directly. Therefore, this system allows easy and fast measurements. The He-MIP-AES is applicable to measurements of not only metals but also halogens and non-metals such as C, Si, and N with high sensitivity due to use of the microwave-induced atmospheric pressure helium plasma emission spectroscopic technique (Haraguchi and Takatsu, 1984; Tanabe, 1985). We have applied He-MIP-AES to the analysis of the GSJ geochemical reference samples and demonstrated the application to the analysis of individual particles. The sample composition, the average particle diameter, and the particle size distribution are already known, so we can compare these data with results obtained by He-MIP-AES to confirm the validity of that technique.

## 2. Experimental

### 2.1. Instrument

The He-MIP-AES Particle Analyzer PT1000 (Yokogawa Electric Co.), was employed to analyze the GSJ geochemical reference samples. The appearance and a schematic diagram of the Particle Analyzer are shown in Figs. 1 and 2, respectively.

The membrane filter was set on a filter holder in the dispersion chamber. The sample particles were delivered into the Beenakker type cavity (Beenakker, 1976) through an aspiration nozzle with helium carrier gas. The condensed particles were released into the individual particles in the sonic velocity region of the aspirator and were introduced into the atmospheric pressure helium plasma individually. The micro-particles were evaporated, atomized, ionized, and excited by the heat of the plasma. The emission pulse data were distributed to the four spectrometers (channels) through optical fibers and processed to detect four different elements simultaneously with 90  $\mu$ sec time resolution. The number of particles, the particle diameters, the elements and the elemental compositions correspond to the number of peaks, the peak intensities, the wavelengths, and the correlation of simultaneous emissions, respectively, in the technique of He-MIP-AES. We have directed our attention to the elemental compositions found from the correlation of simultaneous emissions especially.

We can distinguish a synchronized emission from a non-synchronized one, because those emissions are detected by different spectrometers (channels) simultaneously. Namely, we know if the elements are in one particle or in different particles from the He-MIP-AES (see Fig. 3). The emission intensity is proportional to the particle mass, so the emission intensity is also proportional to the cubes of the particle diameters in the He-MIP-AES.

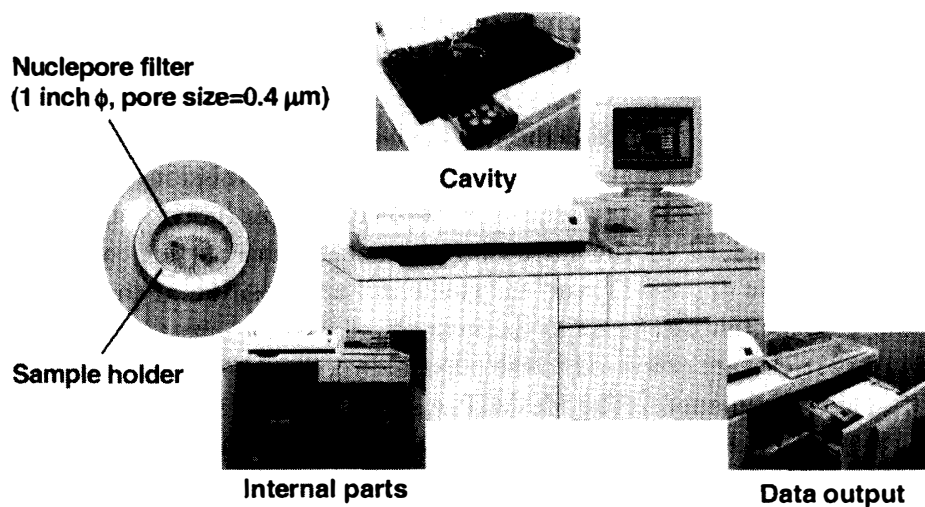


Fig. 1. Appearance of the Particle Analyzer PT1000.

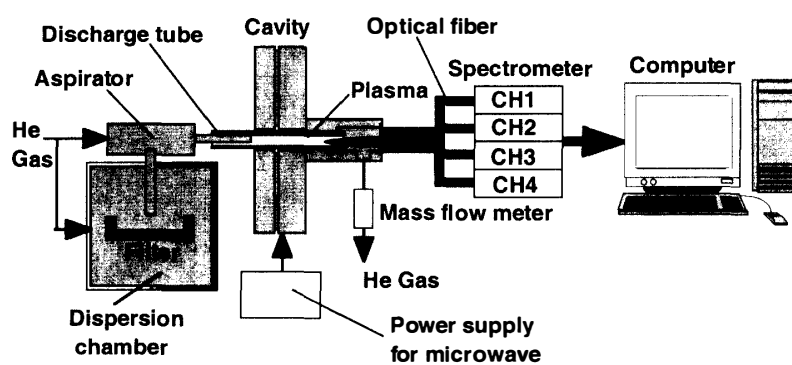


Fig. 2. Schematic diagram of the Particle Analyzer PT1000.

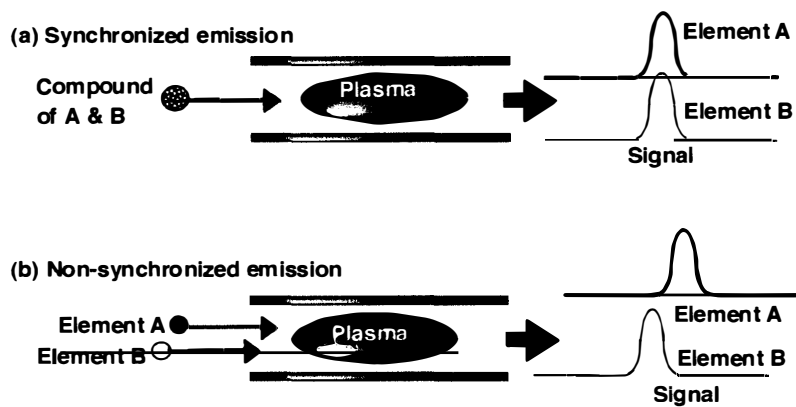


Fig. 3. Schematic illustration of synchronized and non-synchronized emission.

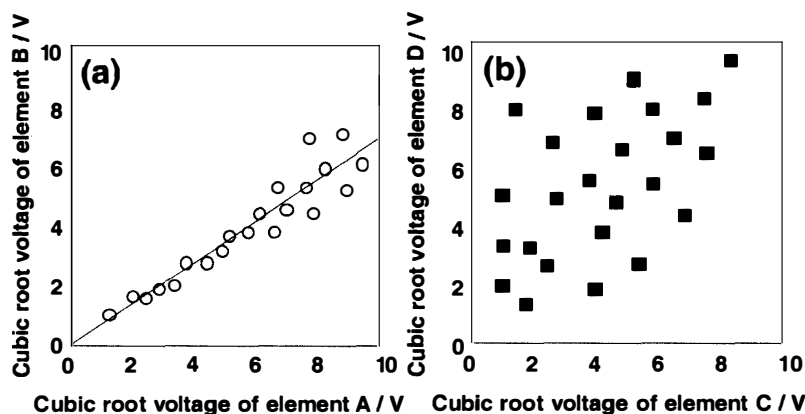


Fig. 4. Two typical patterns of the correlation of cubic root voltage between two different elements for synchronized emission data. (a) There is some correlation between the cubic root voltage of element A and that of element B. (b) There is no correlation between the cubic root voltage of element C and that of element D.

$$D = KI^{1/3}, \quad (1)$$

$D$ : Equivalent particle diameter,

$K$ : Correction coefficient for elemental sensitivity,

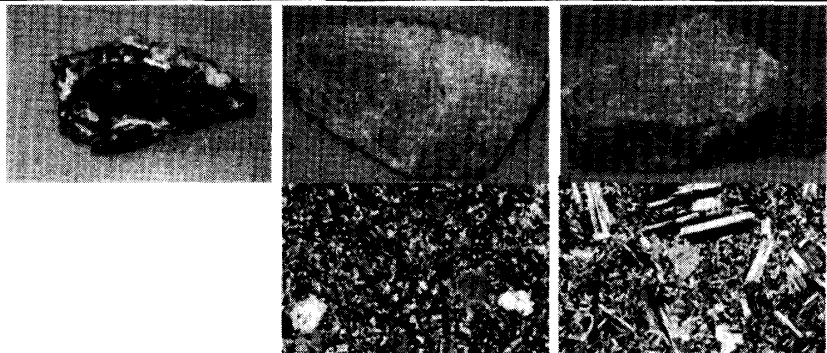
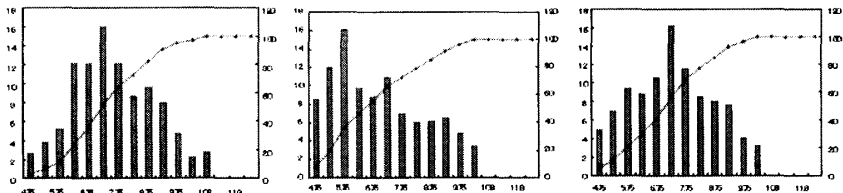
$I$ : Emission intensity.

Therefore, the equivalent particle diameter can be calculated from the cubic root of voltage ( $V$ ) converted from emission intensity with photomultiplier by assuming that the particle is a complete sphere. Figure 4 shows two typical correlation patterns of the simultaneous emission between two different elements. If there is some correlation as shown in Fig. 4a, it means the two elements bond together at a certain ratio, namely, they form a compound. And the slope of the correlation graph is equivalent to the combination ratio between the two elements in the compound. On the other hand, if there is no correlation, as shown in Fig. 4b, it shows coalescent matter. Thus, the He-MIP-AES can provide information about the elemental composition and "equivalent" particle diameter of each particle, and their number and distribution, so this system is an essential tool to know both the character and the origin of particles.

## 2.2. Samples

The geochemical reference samples, JR-1 (rhyolite), JB-1a (basalt), and JB-3 (basalt) were obtained from the Geological Survey of Japan (GSJ). Table 1 shows the compositional and particle size data for the GSJ geochemical reference samples reported by Imai *et al.* (1995). Samples were thoroughly ground by using an agate mortar and collected on a Nuclepore polycarbonate membrane filter (1 inch  $\phi$ , pore size = 0.4  $\mu\text{m}$ ) by a low volume air sampler. The major elements in these rock reference samples, Si, Fe, Ca, and Mg were chosen for analysis. The minor elements in these rock samples, Cr and Ni, were also chosen because the contents of Cr and Ni are very different among the samples (see Table 1).

Table 1. Recommended values for the GSJ reference samples, "Igneous rock series", by Imai *et al.* (1995).

Sample	JR-1 (rhyolite)	JB-1a (basalt)	JB-3 (basalt)	
Collected place	Wada Pass, Nagano Prefecture	Sasebo, Nagasaki Prefecture	Mt. Fuji Yamanashi Prefecture	
Composition	Si (%)	35.27	24.50	23.82
	Fe (%)	0.62	6.33	8.27
	Ca (%)	0.48	6.65	7.00
	Mg (%)	0.07	4.72	3.13
	Cr (ppm)	2.83	392	58.1
	Cu (ppm)	2.68	56.7	194
	Ni (ppm)	1.67	139	36.2
Photo-graph	Appearance			
	Thin section micro-graph			
Particle size distribution				
	Average particle diam.	4.57μ m	9.67μ m	6.49μ m

### 3. Results and discussion

Figure 5 shows the correlation of cubic root of voltage between two different elements for each 5000 synchronized emission data on the GSJ rock samples, JR-1 (red dot), JB-1a (yellow dot), and JB-3 (blue dot), respectively. The major elements in these rock reference samples, Si, Fe, Ca, and Mg were chosen for analysis. Here we defined the cubic root voltage of 1 V as a noise cut level and cut all data less than 1 V in the following correlation graphs. The JR-1 (rhyolite, red dot) has a narrow distribution for all elements in combination in Fig. 5. Especially, there is a clear and strong linear correlation between (a) Si and Fe, (c) Si and Mg, and (e) Fe and Mg, suggesting that Si and Fe, Si and Mg, and Fe and Mg form compounds at certain element ratios for JR-1. On the other hand, the correlations between (a) Si and Fe, (c) Si and Mg, and

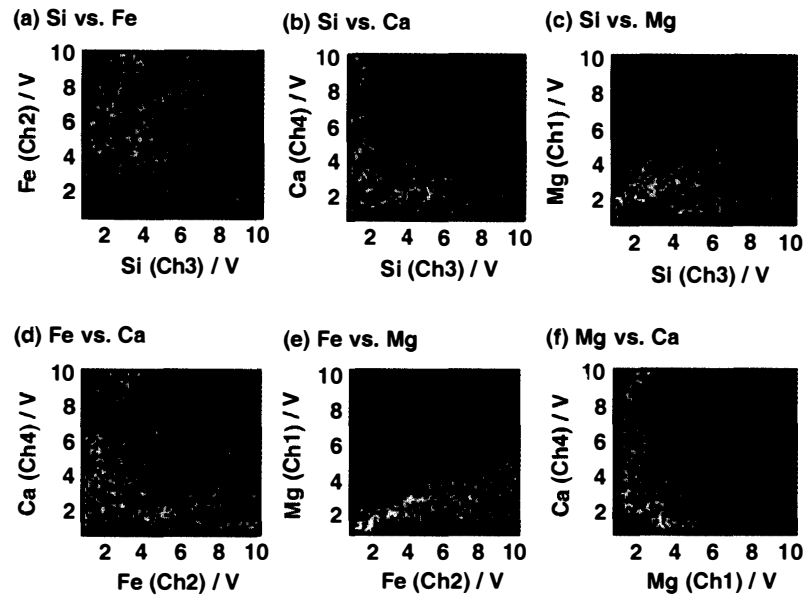


Fig. 5. The correlation of cubic root voltage between two different elements for each 5000 synchronized emission data on the GSJ rock samples, JR-1 (red), JB-1a (yellow), and JB-3 (blue).

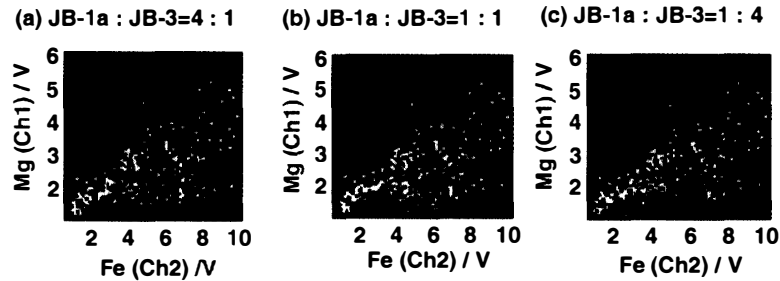


Fig. 6. The correlation of cubic root voltage between iron and magnesium for each 5000 synchronized emission data on the GSJ rock samples, JB-1a (yellow), JB-3 (blue), and their mixture (pink).

(e) Fe and Mg for JB-1a (basalt, yellow dot) and JB-3 (basalt, blue dot), as the same as for JR-1. However, JB-1a and JB-3 have scattered distributions in Figs. 5b, d, and f, respectively. Both JB-1a and JB-3 are classified as basalt, but show different correlation features in Figs. 5c and e. Namely, the slope values are 0.27 (JB-1a, yellow dots) and 0.17 (JB-3, blue dots) in Fig. 5c and 0.38 (JB-1a, yellow dots) and 0.23 (JB-3, blue dots) in Fig. 5e respectively. On the other hand, they have similar dot distributions to each other in Figs. 5a, b, d, and f. Namely, the slope values are 0.77 (JB-1a, yellow dots) and 0.77 (JB-3, blue dots) in Fig. 5a, 0.15 (JB-1a) and 0.17 (JB-3) in Fig. 5b, 0.14 (JB-1a) and 0.11 (JB-3) in Fig. 5d and 0.48 (JB-1a) and 0.45 (JB-3) in Fig. 5f respectively. JB-1a and JB-3 show the different slopes of correlation between Fe and Mg in Fig. 5e (0.38 (JB-1a, yellow dots) and 0.23 (JB-3, blue dots)). This means that Fe and Mg bonds Mg together at different ratios in JB-1a and JB-3, so

we can distinguish between JB-1a and JB-3 by using the slope.

Then, we tried to compare in Fig. 6 this correlation between Fe and Mg for JB-1a (yellow dots), JB-3 (blue dots), and their mixture (pink dots, JB-1a : JB-3 = (a) 4 : 1, (b) 1 : 1, and (c) 1 : 4). JB-1a is major component in the JB-1a : JB-3 = 4 : 1 mixture, so the distribution of pink dots is similar to that of yellow dots (JB-1a) in Fig. 6a. On the other hand, in the case of the JB-1a : JB-3 = 1 : 1 mixture (Fig. 6b), the distribution of pink dots is between that of yellow dots (JB-1a) and blue dots (JB-3). In the case of the JB-1a : JB-3 = 1 : 4 mixture (Fig. 6c), the distribution of pink dots is similar to that of blue dots (JB-3) because JB-3 is the major component in this mixture. This information was obtained by using only 5000 particles and can be measured by using even fewer sample particles. Table 2 shows the minimum sample mass for the He-MIP-AES measurements with the Particle Analyzer PT1000. The minimum sample masses in Table 2 (Yokogawa Electric Corporation, unpublished data) were estimated as follows: the minimum sample "volume" was calculated by cubing the lower limit of detectable "equivalent" particle diameter for each element in the Particle Analyzer system. Then, the minimum sample "weight", namely the minimum sample mass, was derived from the volume and the density. Table 2 indicates that the He-MIP-AES can

Table 2. The minimum sample mass for He-MIP-AES measurements with the Particle Analyzer PT1000.

Elements	Measurable particle size range / $\mu\text{m}$	Minimum mass for measurements / g	Elements	Measurable particle size range / $\mu\text{m}$	Minimum mass for measurements / g
Si	0.76 ~ 7.5	$5.4 \times 10^{-13}$	Mn	0.18 ~ 1.9	$2.3 \times 10^{-14}$
Fe	0.12 ~ 1.3	$7.2 \times 10^{-15}$	Co	0.61 ~ 5.1	$1.0 \times 10^{-12}$
Ni	0.30 ~ 3.1	$1.3 \times 10^{-13}$	Au	0.38 ~ 4.0	$5.7 \times 10^{-13}$
Al	0.49 ~ 3.5	$1.6 \times 10^{-13}$	Mg	0.21 ~ 1.9	$8.3 \times 10^{-15}$
Pb	0.24 ~ 1.8	$8.2 \times 10^{-14}$	V	0.46 ~ 4.6	$3.1 \times 10^{-13}$
Cr	0.39 ~ 3.3	$2.2 \times 10^{-13}$	F	4.90 ~ 20.0	$2.0 \times 10^{-10}$
Cu	0.21 ~ 1.9	$4.3 \times 10^{-14}$	Cl	4.10 ~ 20.0	$7.9 \times 10^{-11}$
C	0.79 ~ 8.3	$5.9 \times 10^{-13}$	S	2.60 ~ 20.0	$1.9 \times 10^{-11}$
Mo	0.45 ~ 3.5	$4.9 \times 10^{-13}$	N	2.40 ~ 20.0	$1.7 \times 10^{-11}$
Ca	0.13 ~ 1.1	$1.8 \times 10^{-15}$	Ag	0.16 ~ 1.7	$2.3 \times 10^{-14}$
W	1.80 ~ 14	$6.0 \times 10^{-11}$	Zr	0.42 ~ 4.2	$2.6 \times 10^{-13}$
B	0.37 ~ 4.1	$6.9 \times 10^{-14}$	P	0.54 ~ 5.8	$1.8 \times 10^{-13}$
Ti	0.56 ~ 4.6	$4.2 \times 10^{-13}$	Ba	0.46 ~ 3.9	$1.8 \times 10^{-13}$
Na	0.43 ~ 2.8	$4.0 \times 10^{-14}$	Ga	0.12 ~ 1.2	$5.1 \times 10^{-15}$
K	1.8 ~ 18	$2.6 \times 10^{-12}$	As	0.26 ~ 2.5	$5.3 \times 10^{-14}$
Zn	0.28 ~ 2.9	$8.2 \times 10^{-14}$	Ce	1.60 ~ 12	$1.4 \times 10^{-11}$

\* The maximum measurable size of 20  $\mu\text{m}$  is limited by the mechanical restriction of Particle Analyzer PT1000.

measure pico or femto grams of samples and supports the results in this study. Namely, the He-MIP-AES technique should be applicable for the analysis of individual particulate matter, such as the ancient tephra particles in the Dome Fuji deep ice core.

Figure 7 shows the sum of emission intensities for 3000 particles on JB-1a, and JB-3 and their mixtures (JB-1a : JB-3 = 4 : 1 and 1 : 4), respectively. We chose Cr and Ni, the minor elements in these samples, because the content ratios of Cr and Ni are very different between JB-1a and JB-3, as shown in Table 1. The sums of Cr and Ni emission intensities are shown as black and gray bars with the left axis. In Fig. 7, the sum of emission intensities is normalized by dividing by the sum of Si emission intensities, because silicon is a matrix of these rock particles and the content ratio is almost the same between JB-1a and JB-3. This treatment was performed to avoid influencing of the result by the weight difference in each 3000 particles, since the 3000 particles always do not weigh exactly the same.

The content ratio of Cr and Ni against that of Si, calculated from the values in Table 1, are compared in Fig. 7. At first, we expected to distinguish between JB-1a and JB-3 by comparing the sum of emission intensities for Cr and/or Ni to their content ratio. It seems that the sum of Ni emission intensities is proportional to the content ratio of Ni (dotted line with the right axis) and there is some relationship between the sum of Cr emission intensities and the content ratio of Cr (solid line with the right axis) in Fig. 7. These facts, however, are not conclusive identify the origin of particles.

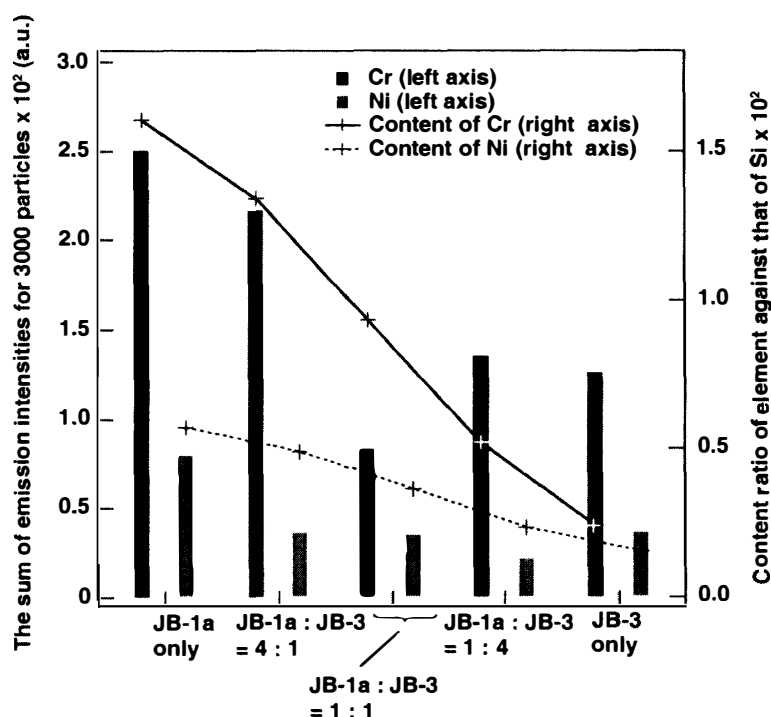


Fig. 7. The sum of emission intensities for 3000 particles on the GSJ rock samples, JB-1a, JB-3, and the mixtures (JB-1a : JB-3 = 4 : 1, 1 : 1, and 1 : 4). The sum of Cr and Ni emission intensities (normalized by dividing into the sum of Si emission intensities, respectively) are shown as black and gray bars with the left axis. The content ratios of Cr and Ni against that of Si are shown as a solid line and a dotted line with the right axis.



One of the reasons for this inconsistency may be that the cubic roots of voltages less than 1 V were automatically neglected as noise in this system. The sum of emission intensities for an element contained in small particles must be underestimated. We must discuss how to treat information such as that shown in Fig. 7 in the future.

#### 4. Summary

The individual micro-particles of the GSJ geochemical reference samples were analyzed for their elemental composition by the He-MIP-AES. The JB-1a and JB-3 samples gave different characteristic correlations of the cubic root voltage for simultaneous emission elements, respectively, even though both JB-1a and JB-3 are classified as basalt. This suggests that we can characterize micro-particles by measuring the correlation of simultaneous emissions for the individual particles and analyzing the distinctive features of their correlations for all particles. Namely, the He-MIP-AES technique should be applicable for the identification of individual particulate matter, such as tephra particles.

#### Acknowledgments

The authors are grateful to Dr. N. Imai (Geochemistry Section, Geological Survey of Japan (GSJ), National Institute of Advanced Industrial Society and Technology (AIST), Ministry of Economy) for a gift of the GSJ geochemical reference samples. The authors wish to thank Dr. K. Takeuchi (Argonne National Laboratory, U.S.A.) for reading the manuscript.

#### References

- Beenakker, C.I.M. (1976): A cavity for microwave-induced plasmas operated in helium and argon at atmospheric pressure. *Spectrochim. Acta*, **31B**, 483–486.
- Imai, N., Terashima, S., Itoh, S. and Ando, A. (1995): 1994 Compilation for GSJ reference samples. *Geochem. J.*, **29**, 91–95.
- Hara, K., Kikuchi, T., Furuya, K., Hayashi, M. and Fujii, Y. (1996): Characterization of Antarctic aerosol particles using laser microprobe mass spectrometry. *Environ. Sci. Tech.*, **30** (2), 385–391.
- Haraguchi, H. and Takatsu, A. (1984): Atmospheric pressure helium microwave-induced plasma emission spectrometry. *Bunseki*, **2**, 108–114 (in Japanese).
- Kudo, Y., Nakamura, H., Suzawa, T., Furuya, K., Kikuchi, T., Kamiyama, K. and Watanabe, O. (2000): Evaluation of contamination in preparation of an Antarctic ice core for microparticle analysis with SEM-EDX. *Polar Meteorol. Glaciol.*, **14**, 34–46.
- Takahara, H. (1993): Elemental analysis for particles using microwave induced plasma. *Ultra Clean Technol.*, **5** (4), 310–318 (in Japanese with English abstract).
- Tanabe, K. (1985): Atmospheric pressure helium microwave-induced plasma emission spectrometry. *Bunseki*, **6**, 390–396 (in Japanese).
- Wouters, L., Artaxo, P. and Van Grieken, R. (1990): Laser microprobe mass analysis of individual Antarctic aerosol particles. *Int. J. Environ. Anal. Chem.*, **38**, 427–438.

*(Received February 15, 2001; Revised manuscript accepted August 2, 2001)*